

COOL CUSTOMERS IN THE STELLAR GRAVEYARD II: LIMITS TO SUBSTELLAR OBJECTS AROUND NEARBY DAZ WHITE DWARFS

JOHN H. DEBES¹, STEINN SIGURDSSON¹, BRUCE E. WOODGATE²

Draft version June 29, 2018

ABSTRACT

Results from a concerted Hubble Space Telescope (HST) survey of nearby white dwarfs for substellar objects is presented. A total of 7 DAZ white dwarfs with distances of < 50 pc had high contrast and high spatial resolution NICMOS coronagraphic images taken to search for candidate substellar objects at separations $\lesssim 10''$ away. Limits to unresolved companions are derived through analysis of 2MASS photometry of the white dwarfs compared to expected fluxes based on the WDs effective temperature, distance, and gravity. Our HST survey of seven DAZ white dwarfs identified candidate companions for four of the white dwarfs. For three of these four, HST and ground-based second epoch observations showed the candidates to be background stars. The fourth white dwarf, which is close to the galactic plane, has seven candidate companions at distances of $2''$ to $4''$, which remain to be followed up. We find that for four of the white dwarfs we are sensitive to planetary companions $\gtrsim 10 M_{Jup}$. For all of the targets, we are sensitive to companions $> 18 M_{Jup}$. The lack of significant near infrared excesses for our targets limits any kind of unresolved companions present to be substellar. In light of these results we make several comments on the possibility of determining the origin of metals in the atmospheres of these white dwarfs.

Subject headings: circumstellar matter — planetary systems — white dwarfs — stars: low-mass, brown dwarfs — infrared:stars

1. INTRODUCTION

The last ten years have shown a surge of new discoveries about objects of substellar mass. Radial velocity surveys of main sequence K-F stars have found few brown dwarf companions at separations of < 3 AU, but a profusion of planetary mass companions (Marcy & Butler 2000). Large all sky-surveys, such as 2MASS and SDSS have found large numbers of free floating brown dwarfs (Burgasser et al. 2003; Hawley et al. 2002). Low mass substellar objects down to planetary mass have been discovered in young clusters such as σ Orionis (Lada & Lada 2003, and references therein). At the same time, imaging surveys of nearby main sequence stars have found several substellar companions thanks to high contrast imaging (e.g. Forveille et al. 2004). One population of stars which still has little data are intermediate mass stars with masses between $1.5\text{--}8 M_{\odot}$.

The reason for the dearth of information around intermediate mass stars is two-fold. First, the majority of searches for planetary systems focus on Solar System analogues. Secondly, there are technical limitations to searching for planets and brown dwarfs around main sequence F-B stars. Radial velocity surveys rely on a large number of narrow absorption lines in the stellar spectrum to achieve high precision velocity measurements (Delfosse et al. 1998; Griffin et al. 2000). As the effective temperature of a star increases, metal line strengths decrease and there are fewer lines for measurement. Stars with higher masses have a correspondingly smaller reflex motion due to a low mass companion. Radial velocity surveys of G giant stars can probe higher mass stars, but there are only two planetary candidates currently

reported (Sato et al. 2003; Setiawan et al. 2005). More massive stars have higher luminosities as well, making high contrast imaging more limited in its effectiveness if one is looking for the thermal emission from a companion. Reflected light from substellar companions is most useful within a few AU of a star and is negligible at larger distances (Burrows et al. 2004). In most cases, searches focus on detecting the thermal radiation from a substellar companion.

The effects of higher intrinsic luminosity are illustrated by noting the sensitivity to substellar companions of the NICMOS instrument on HST. High contrast imaging can achieve $\Delta H \sim 10$ at $1''$ on the NICMOS coronagraph with PSF subtraction, allowing $45 M_{Jup}$ mass companions to be detected around a 1 Gyr solar mass star. For an A star with a mass of $2 M_{\odot}$ at 1 Gyr, a $90 M_{Jup}$ companion can be detected. Finally, more massive stars are rarer in local space, forcing observations of young star forming regions at larger distances.

Recent images of young HAe/Be stars with circumstellar disks such as HD 141569, HR 4796A, and AB Aurigae motivate a search for planets around higher mass stars (Weinberger et al. 1999; Jayawardhana et al. 1998; Grady et al. 1999). Sub-mm observations of warped and clumpy disks around stars such as Vega and Formalhut show that planet formation may be vigorous for higher mass central stars (Holland et al. 1998). What is still unclear is how planet formation efficiency varies with stellar mass and whether the brown dwarf desert is present over the same orbital separations for higher mass stars.

The 145 or so discoveries of planets by radial velocity surveys have told us much about planet formation, but discoveries of planets in orbit around post main sequence objects have the opportunity to challenge many accepted assumptions developed on the basis of our current knowledge. For example, the first terrestrial planets

¹ Department of Astronomy & Astrophysics, Pennsylvania State University, University Park, PA 16802

² NASA Goddard Space Flight Center, Greenbelt, MD 27710

TABLE 1
PROPERTIES OF THE TARGET WHITE DWARFS

WD	Name	M_f^a (M_\odot)	T_{eff} (K)	t_{cool} (Gyr)	D (pc)	M_i (M_\odot)	$t_{cool} + t_{MS}$ (Gyr)	References
0208+396	G 74-7	0.60	7310	1.4	17	2.1	3.2	1
0243-026	G 75-39	0.70	6820	2.3	21	3.2	2.8	1
0245+541	G 174-14	0.76	5280	6.9	10	4.6	7.2	1
1257+278	G 149-28	0.58	8540	0.9	34	1.7	3.3	1
1337+701	EG 102	0.57	20435	0.1	25	1.6	3.3	2,3
1620-391	CD-38°10980	0.66	24406	0.1	12	3.1	0.7	4
2326+049	G 29-38	0.70	11820	0.6	14	3.7	1	2,5

REFERENCES. — (1) Bergeron et al. (2001) (2) Liebert et al. (2005) (3) Perryman et al. (1997)
(4) Bragaglia et al. (1995) (5) van Altena et al. (2001)

^aValues for M_f , T_{eff} , and t_{cool} were determined from listed references. Distances derived from parallax measurements compiled in (1). If not available, (3) and (5) were used. See Section 5.2 for the calculation of M_i and the WDs' total ages.

ever discovered were around a pulsar (Wolszczan & Frail 1992). The oldest Jovian planet discovered in the M4 globular cluster in orbit around a white dwarf demonstrates that planet formation can occur in metal poor systems (Sigurdsson et al. 2003). This discovery must be explained in the context of planet formation mechanisms that favor stars with higher metallicity.

Detecting substellar companions in orbit around white dwarfs have several advantages compared to searching main sequence stars. Given their intrinsic dimness, white dwarfs allow high contrast searches to probe interesting orbital separations (Burleigh et al. 2002). In addition, their higher effective temperature allows searches for unresolved excesses at longer wavelengths (Ignace 2001). Given the range of progenitor masses, white dwarfs probe a large range of stellar mass. Finally, they complement radial velocity and transit searches that are biased towards close companions. High spatial resolution and high contrast imaging in the near infrared with the NICMOS camera on HST allows the best chance for detecting faint cool companions to nearby white dwarfs. Planetary mass objects that are less than 3 Gyr can be observed in the near-IR, specifically in the F110W (\sim J) and F160W (\sim H) filters. For example, a 3 Gyr old $10 M_{Jup}$ planet can be observed out to 20 pc with an HST observation of \sim 1200s.

Searching a subset of white dwarfs that harbor markers for substellar objects can maximize the return of a survey. Nearby hydrogen white dwarfs with metal line absorption (DAZs) may fit this criterion. Three hypotheses have been put forth to explain the presence of DAZs: interstellar matter (ISM) accretion (Dupuis et al. 1992, 1993a,b), unseen companion wind accretion (Zuckerman et al. 2003), and accretion of volatile poor planetesimals (Alcock et al. 1986; Debes & Sigurdsson 2002; Jura 2003).

ISM accretion has a wealth of problems in predicting many aspects of DAZs such as the large accretion rates required for some objects and the distribution of these objects with respect to known clouds of dense material (Aannestad et al. 1993; Zuckerman & Reid 1998; Zuckerman et al. 2003). The quick atmospheric settling times of hydrogen atmospheres imply that the white dwarfs are in close proximity with accretionary material.

Of the \sim 34 DAZs known, seven of them have dM companions, supporting the argument that DAZs could have unseen companions that place material onto the WD surface through winds (Zuckerman et al. 2003). In order to accrete enough material, companions must be in extremely close orbits, bringing into question why these objects have yet to be discovered through transits, radial velocity surveys of compact objects, or observable excesses in near-IR flux. In most cases the reflex motion from such objects would be easily detectable (Zuckerman & Becklin 1992). The idea of the presence of unseen companions also cannot explain objects like WD 2326+049 (G 29-38) which has an infrared excess due to a dust disk at roughly the tidal disruption radius (Graham et al. 1990; Patterson et al. 1991).

The invocation of cometary or asteroidal material as a method of polluting WD atmospheres was developed to explain photospheric absorption lines due to metals in the DAZ WD 0208+395 (G 74-7) (Alcock et al. 1986). However, the rates predicted by these original studies could not satisfactorily explain the highest accretion rates inferred for some objects and could not easily reproduce the distribution of DAZs based on their effective temperatures (Zuckerman et al. 2003). However, mixing length theory predicts a drop-off of observability for accretion as a function of effective temperature which may swamp out the earlier prediction of Alcock et al. (1986) (Althaus & Benvenuto 1998). Also unclear is the effect non-axisymmetric mass loss could have on the fraction of comet clouds lost by their hosts during post main sequence evolution (Parriott & Alcock 1998). By hypothesis, cometary clouds are the result of planet formation, so the long term evolution of planetary systems and their interaction with these comet clouds needs to be investigated (Tremaine 1993).

The problems of the Alcock et al. (1986) model can be overcome by studying the stability of planetary systems during evolution of the central star as it undergoes mass loss, leaving the main sequence and evolving into a white dwarf. Most planetary systems are stable on timescales comparable to their current age. During adiabatic mass loss, companions expand their orbits in a homologous way, increasing their orbital semi-major axes by a factor M_i/M_f (Jeans 1924). This change in the central stellar

mass affects the dynamics of the planetary system.

The change in stellar mass specifically affects the stability planetary systems, typified by the Hill stability criterion against close approaches for two comparable mass planets. The stability criterion is roughly described as $\Delta_c = (a_1 - a_2)/a_1 = 3\mu^{1/3}$, where a is the semi-major axis, μ is the mass ratio of the planets to the host star, and Δ_c represents the critical separation at which the two planets become unstable to close approaches (Hill 1886; Gladman 1993). The critical separation grows as the relative separation of the two planets stays the same, resulting in marginally stable systems being tipped over the edge of stability. This instability can lead to orbital rearrangements, the ejection of one planet, and collisions (Ford et al. 2001). These three events dramatically change the dynamical state of the planetary system, leading to a fraction of systems that perturb the surviving comet cloud and sending a shower of comets into the inner system where they tidally disrupt, cause dust disks, and slowly settle onto the WD surface. This modification of the comet impact model can explain the accretion rates needed for the highest abundances of Ca observed and the presence of infrared excesses around WDs (Debes & Sigurdsson 2002).

For two of the three above explanations, unseen planetary or substellar objects lurk in the glare of nearby white dwarfs with metal lines in their atmospheres. DAZs represent a promising population for a search for cool objects in orbit around WDs. If such companions can be detected, this will open an exciting chapter in the study of extra-solar planets by presenting several objects that can be directly detected and characterized, constraining a host of theoretical issues, such as extra-solar planetary atmospheres and the long term evolution of Jovian planets. Such observations in the stellar graveyard can support future missions dedicated to the detection and characterization of terrestrial planets. White dwarfs represent an intermediate step between our current technology and what is needed for observations made with the James Webb Space Telescope (JWST) and the Terrestrial Planet Finder (TPF). Coupled with the possible marker of metal absorption, a sample of nearby stars easier to study than main sequence stars guaranteed to have some sort of planetary system could enhance the efficiency of such long term searches and may provide extra clues to the nature of planet formation.

To that end, we were motivated to search the seven brightest and closest DAZ white dwarfs with the NIC-2 coronagraph on the NICMOS instrument of the Hubble Space Telescope (HST). This search was part of the the Cycle 12 program 9834, completed over the course of 2003 and 2004 with 14 orbits. The first results from this survey focused on WD 2326+049 (G 29-38), a DAZ with an infrared excess (Debes et al. 2005b, hereafter DSW05). We present the observations we made in Section 2 and detail our data analysis in Section 3. We present candidate planetary and brown dwarf companions in Section 4 as well as place limits on the types of candidates we could have detected in Section 5. Finally, we discuss the implications of our work and lay out future possibilities in Section 6.

2. OBSERVATIONS

Only \sim 34 DAZs are currently known to exist, since the detection of their weak metal lines are difficult without a high signal-to-noise, high resolution spectrograph (Zuckerman et al. 2003). Six of the most promising DAZ white dwarfs discovered or confirmed in the Zuckerman et al. (2003) survey were targeted for observation with NICMOS and are listed in Table 1. Our seventh target, WD 1620-391, was chosen for the presence of circumstellar gas absorption features as well as photospheric absorption due to Si and C (Holberg et al. 1995). We chose these targets based on the fact that these were the brightest and closest DAZs known. Each target was observed with the NIC-2 coronagraph in the F110W filter. The most promising targets, WD 2326+049, WD 1337+701, and WD 1620-391 were imaged in the F160W filter as well. With the exception of the newly discovered DAZ GD 362, both WD 2326+049 and WD 1337+701 have the highest [Ca/H] abundances measured (Gianninas et al. 2004). WD 1620-391 was chosen for extra observations due to the presence of its circumstellar material. These three targets were also observed without the coronagraph for shorter exposures in the F110W, F160W, and F205W filters in an attempt to resolve any smaller structure or companions at separations $< 0.8''$. Acquisition images were used for the other targets. Following the prescription of Fraquelli et al. (2004), two coronagraphic exposures of \sim 600 s were taken at two different spacecraft roll angles. Each exposure was separated by a differential roll angle of 10° . The differential roll angle between images limits the angular separation at which one can detect a point source, requiring at least a two pixel separation between the centroids of the positive and negative conjugates to avoid the self subtraction of any point source companions. This requirement is tempered by the need to spend most of the HST orbit observing the target and not rolling the spacecraft. For our observations, we concentrated on integration time and chose a roll angle of 10° , leading to an inner radius limit to extreme high contrast imaging with self subtraction of $0.86''$.

Table 2 shows a log for all of the observations taken along with the total exposure times and the filter used. Each F110W observation was designed to be sensitive enough to detect an object with $m_{F110W} \sim 23$ with a S/N of 10, which for a 1 Gyr substellar object at 10 pc would correspond to a $\sim 5 M_{Jup}$ planet. For our seven targets, which range in age from 1 Gyr to 7 Gyr and 10 to 34 pc, we are sensitive to $7-18 M_{Jup}$ objects.

In addition to the seven targets, three reference stars were imaged with the three WDs observed without the coronagraph. The goal was to use these to subtract out the point spread function (PSF) that can obscure fainter objects or dust disks. These targets were chosen to be close to the original target and have similar near-IR colors to aid in PSF subtraction. No close companions or structure were detected using the reference stars.

One group of observations taken of WD 0245+541 failed due to an incorrect calibration onboard the telescope, with the flight software (FSW). As a result, WD 0245+541 was not placed behind the coronagraphic hole. The problem was identified by the HST staff and further observations did not show the same problem. A repeat observation was taken in October 2004, but the original failed observations were also used for our data analysis.

TABLE 2
TABLE OF HST OBSERVATIONS

WD	Observation Group	Date & Time (UT)	Integration Time	Filter
0208+396	N8Q320010	2003-09-15 19:42:00	575.877	F110W
	N8Q322010	2003-09-15 20:10:00	575.877	F110W
0243-026	N8Q322010	2003-09-18 18:11:00	575.877	F110W
	N8Q323010	2003-09-18 18:39:00	575.877	F110W
0245+541	N8Q318010	2003-08-26 21:11:00	575.877	F110W
	N8Q319010	2003-08-26 21:39:00	575.877	F110W
1257+278	N8Q368010	2004-10-24 07:45:00	575.877	F110W
	N8Q369010	2004-10-24 09:11:00	575.877	F110W
1337+701	N8Q316010	2004-02-18 11:12:00	575.877	F110W
	N8Q318010	2004-02-18 11:41:00	575.877	F110W
1620-391	N8Q302010	2003-12-01 17:09:00	25.918	F205W
	N8Q302011	2003-12-01 17:11:00	25.918	F205W
	N8Q302020	2003-12-01 17:20:00	21.930	F160W
	N8Q302030	2003-12-01 17:24:00	19.936	F110W
	N8Q308010	2004-02-05 21:40:00	575.877	F110W
	N8Q309010	2004-02-05 22:45:00	575.877	F110W
	N8Q310010	2004-02-05 23:13:00	575.877	F160W
	N8Q311010	2004-02-06 00:27:00	575.877	F160W
	N8Q303010	2003-09-07 06:12:00	23.924	F205W
	N8Q303011	2003-09-07 06:13:00	23.924	F205W
2326+049	N8Q303020	2003-09-07 06:22:00	17.942	F160W
	N8Q303030	2003-09-07 06:25:00	15.948	F110W
	N8Q312010	2004-03-08 03:22:00	575.877	F110W
	N8Q313010	2004-03-08 03:52:00	575.877	F110W
	N8Q314010	2004-03-08 05:00:00	575.877	F160W
	N8Q315010	2004-03-08 05:27:00	575.877	F160W
	N8Q301010	2003-10-20 10:07:00	17.942	F205W
	N8Q301011	2003-10-20 10:08:00	17.942	F205W
	N8Q301020	2003-10-20 10:15:00	11.960	F160W
	N8Q301030	2003-10-20 10:20:00	11.960	F110W
	N8Q304010	2003-09-14 19:31:00	575.877	F110W
	N8Q305010	2003-09-14 19:59:00	575.877	F110W
	N8Q306010	2003-09-14 21:07:00	575.877	F160W
	N8Q307010	2003-09-14 21:35:00	575.877	F160W

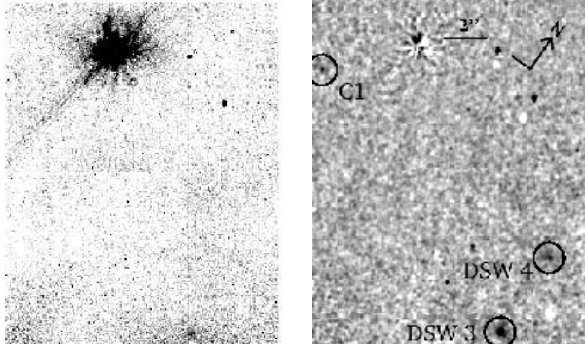


FIG. 1.— Image of WD 2326+049 in the F160W filter before (left) and after (right) PSF subtraction. The right panel has been Gaussian smoothed to show a candidate and two extragalactic objects. Other dark features not marked are detector defects.

Due to the detection of a candidate planetary candidate around WD 2326+049 (G 29-38), second epoch observations were taken with the Gemini North Telescope using the Altair adaptive optics system in conjunction with the NIRI camera. Altair can successfully guide on stars with $R \sim 13$, such as WD 2326+049. By concentrating a diffraction limited fraction of the total flux of a dim object, the background can be overcome for extremely faint near infrared point sources. In addition, under decent observing conditions, the full width at half-maximum

(FWHM) of the core on Altair images is $\sim 60\text{-}90$ mas, providing the possibility to resolve structures better than HST (Hutchings et al. 2004).

The Gemini observations were taken on August 5, 2004. A total of 4×15 s frames were co-added at 10 dither points to subtract the background and to remove pixel to pixel defects, for an effective integration on source of forty minutes. Our total integration returned an average FWHM of 75 mas, significantly smaller than the diffraction limit of our F110W images with HST.

3. DATA ANALYSIS

Data was reduced by the calibration pipeline provided for NICMOS. In addition to the pipeline, certain steps were taken in an effort to improve the quality of the final images, roughly following the procedure set out by Fraquelli et al. (2004). Each 600 s exposure was broken up into two or three exposures for ease in rejecting cosmic rays. Each calibrated subexposure had pedestal subtraction by the PEDSUB routine in IRAF through the STSDAS package. Each subexposure was registered and median combined with sigma clipping to create a final exposure at a particular roll angle. The two images at different roll angles were subtracted one from the other and vice versa to create two difference images: a ROLL1-ROLL2 image and a ROLL2-ROLL1 image. One difference image was rotationally registered and median combined to produce the final total image. Figure 1 shows the before and after pictures of a subtraction shown at

the same image stretch. The residual light due to the coronagraphic PSF is dominated by systematic errors, but in general is a factor of 20-50 times dimmer after subtraction.

In the case of WD 0245+541, several other steps had to be taken for the failed observation since at each roll angle the star was at a different position and not behind the coronagraphic hole. To combat the poor positions, the two images were registered and difference images were produced. The final result was of sufficient quality to determine the presence of several candidate objects in the field.

4. CANDIDATE COMPANIONS AND EXTRAGALACTIC OBJECTS

Of the seven targets, only four showed candidate companions in their fields. The rest did not show anything with the exception of WD 1257+278, which had a resolved galaxy in the background. Any extended objects were interpreted to be background objects and all point sources were flagged as potential companions. Where second epoch images were available with 2MASS or the POSS survey, they were used or second observations were taken. Each candidate with second epoch images was checked for common proper motion with the target WD by measuring the relative radius and pointing angle in degrees East of North of the companion. Extragalactic objects could potentially be of interest due to their proximity to a bright object that could be used for guiding in a laser AO system or multi-conjugate AO system.

The second epoch Gemini data was processed using several IRAF tasks designed by the Gemini Observatory and based upon the sample scripts given to observers. Each frame was flatfielded and sky subtracted. In addition, due to the on-sky rotation from the Cassegrain Rotator being fixed, each frame was rotationally registered and combined.

To determine if an object had common proper motion with a target WD, we calculated the predicted motion of the WD on the sky based on its proper motion. When comparing possible companions with 2MASS or POSS data, proper motion alone was sufficient to determine objects that were in the background. For WD 2326+049, WD 1620-391, and WD 0245+541, the annual parallactic motion of the star was also calculated for an added means of determining background point sources. Any object in orbit around a WD would also have to share both proper motion and annual parallactic motion.

It is also important to adequately understand the errors in order to detect any possible proper motion of the background object or to determine how significant a measure of common proper motion is. The greatest sources of error are due to uncertainties in the parallax of the WD, proper motion, and centroiding errors in the PSF of the candidate. Centroiding errors for faint sources can be determined by looking at images in two filters for one of our fields that has a lot of background sources. The field of WD 1620-391 has several background point sources that can be compared between filters and two epochs. Comparing the difference of ~ 30 sources between the F110W and F160W filters of the observation sets of N8Q312010 and N8Q314010 yields a standard deviation between sources of ~ 10 mas, which we will adopt as our general centroiding error.

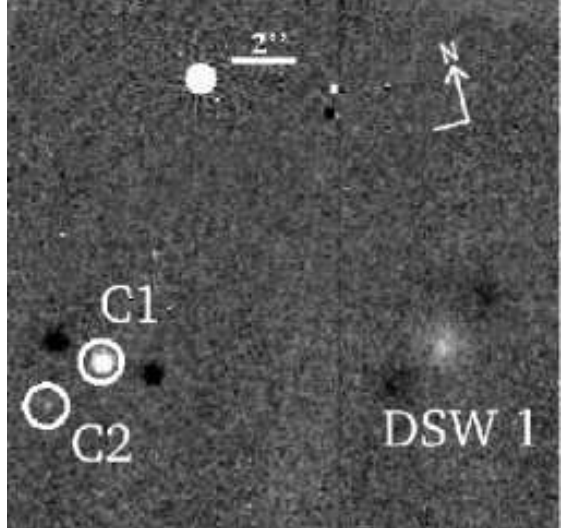


FIG. 2.— Field of WD 0208+395 with its candidates. Candidates are circled and the WD is masked to hide the systematic subtraction errors. A galaxy is detected in the lower right of the image.

4.1. WD 2326+049

Figure 1 shows the NICMOS field of view around this WD, which included a candidate planetary companion, that we designated C1. In addition, there were two faint extended galaxies in the field. C1 is discussed in more detail in DSW05 and has been confirmed to be a background object with a second epoch observation with the Gemini North Altair+NIRI instrument. If this object had been associated, its F110W and F160W magnitudes were consistent with a $7 M_{Jup}$ object. Table 3 presents all the extragalactic objects discovered in this survey along with their positions and apparent Vega magnitudes in the F110W and F160W filters

4.2. WD 0208+395

Figure 2 shows two candidate objects, C1 and C2 and a galaxy in the field of WD 208+395. Since the separation between these objects and WD 208+395 were greater than a few arcseconds, we pursued a second observation with the Canada France Hawaii Telescope with the PUEO+KIR instruments. A second epoch image shows that both C1 and C2 are in the background. This result is discussed in detail in Debes et al. (2005a). If they had been associated, C1 was consistent with a 3 Gyr old $15 M_{Jup}$ brown dwarf and C2 consistent with a $10 M_{Jup}$ planet.

4.3. WD 0245+541

This object, due to its failed first observation, was re-imaged \sim one year later (see Table 1) which provided an ample baseline to test candidates for common proper motion. Figure 3 shows the surrounding area of WD 0245+541, along with three candidates in the field. C1 appears to be a binary object at a distance of $\sim 3''$ which in the second epoch image is clearly not co-moving. C2 is at a separation of $\sim 6''$ and 270° PA. Inspection of the POSS2 red image of this field clearly shows a point source at a separation consistent with this object being a background source. Finally, C3 has a separation

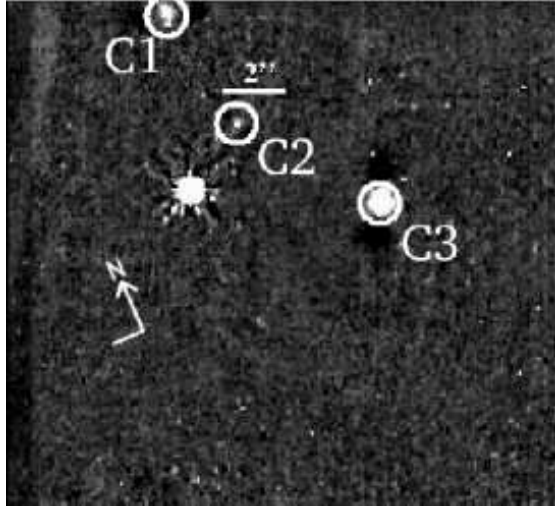


FIG. 3.— Field of WD 0245+541 with its candidates circled.

of $2.5 \pm 0.02''$ and $348 \pm 1^\circ$ PA. WD 0245+541 has a predicted motion between the two epochs of -667 mas and -475 mas, leading to a predicted $\Delta\alpha = 0.17 \pm 0.12''$ and $\Delta\delta = 2.94 \pm 0.12''$ if C3 is non co-moving, compared to the observed $\Delta\alpha = 0.07$ and $\Delta\delta = 2.86$. The candidate does not have common proper motion, and is therefore a background object. The main source of error was in the reported proper motion, which had quoted errors of $0.1''/\text{yr}^{-1}$ (Bakos et al. 2002). If C3 had been associated, its F110W magnitude would have been consistent with an $18 M_{Jup}$ brown dwarf companion.

4.4. WD 1620-391

WD 1620-391 resides quite near the galactic plane and as such has an extremely crowded field with ~ 36 sources of varying brightnesses, which can be seen in Figure 4. Any possible companion must be separated from background objects. A viable candidate in this field would have to be selected by an F110W-F160W color being consistent with a substellar object. Since most of these objects are background objects we must first see if there is any evidence to suspect that there would be a candidate in this field rather than assuming that all sources were background objects. The number of objects as a function of distance should be $\propto r^2$ if the background distribution is truly random. A different distribution would be caused either by the presence of objects physically associated to the central white dwarf or due to physical associations among background stars, such as binaries or clustering. To look for a departure from the expected distribution, we plotted the number of sources in the WD1620-391 field as a function of radial distance from the WD as shown in Figure 5. We compared this distribution to a pure r^2 distribution through means of a K-S test. We find that there is a 97% probability that the distribution is not based on the r^2 distribution mainly due to the hump of sources present close to the WD. We believe that those objects are viable candidates and that in a statistically significant way the distribution of sources $< 4''$ is fundamentally different than what would be expected. A caveat, however, is that since the WD is at a low galactic latitude the statistical test may merely

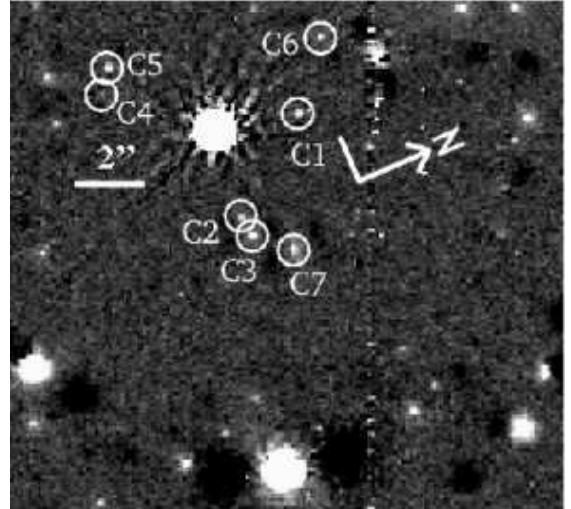


FIG. 4.— Field of WD 1620-391 with its candidates. Each candidate that is circled is within $4''$ and has colors consistent within the photometric errors to a candidate planetary object.

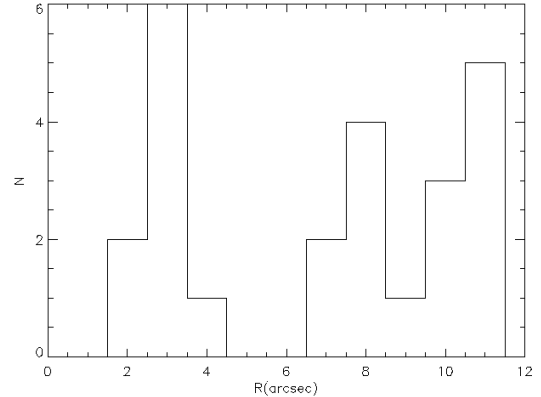


FIG. 5.— Distribution of point sources as a function of distance around the white dwarf WD 1620-391.

be detecting some fundamental structure in the background sources rather than the presence of a candidate. Additionally, the scenario of Debes & Sigurdsson (2002) would predict more than one planet in the system to efficiently slingshot comets or asteroids to the surface of the white dwarf, so the potential exists that two planetary candidates could be present in this “hump” of sources $< 4''$.

Regardless, we have plotted all the detected sources in a CMD and compared them to a predicted isochrone of substellar objects in Figure 6. The WDs age is ~ 1 Gyr so we used the 1 Gyr models of Burrows et al. (2003) convolved with the HST filters. There are some candidates that are within $4''$ and who have colors consistent within the errors to be a planetary candidate. Table 4 lists the candidates, their magnitudes in F110W and F160W. Every one of the candidates would be $\sim 5\text{-}6 M_{Jup}$ in mass if associated. This WDs proper motion is ~ 75 mas/yr in RA and ~ 0 mas/yr in Dec (Perryman et al. 1997), so a second epoch image will be necessary in ruling out any of these sources.

While we have two sets of observations for WD 1620-391 separated by six months, our first image is not sen-

TABLE 3
TABLE OF EXTRAGALACTIC OBJECTS

DSW #	RA	Dec	F110W	F160W	Notes
1	02 11 20.51	+39 55 14	21.36 \pm 0.04		
2	12 59 45.63	+27 34 01	22.8 \pm 0.1		$\sim 1.4''$ extent
3	23 28 47.96	+05 14 38	23.7 \pm 0.2	22.1 \pm 0.1	0.23'' aperture
4	23 28 47.67	+05 14 40	24.0 \pm 0.2	22.8 \pm 0.2	0.23'' aperture

TABLE 4
CANDIDATES AROUND WD1620-391

Candidate	R	PA	F110W	F160W
C1	2.22'' \pm 0.09	328.5 \pm 0.7	22.9	21.6
C2	2.56'' \pm 0.13	262 \pm 5	22.9	21.8
C3	3.10'' \pm 0.10	265 \pm 3	22.4	21.0
C4	3.13'' \pm 0.14	141 \pm 1	23.9	23.0
C5	3.24'' \pm 0.12	129.6 \pm 0.8	22.7	21.5
C6	3.63'' \pm 0.17	27 \pm 2	22.5	21.2
C7	3.91'' \pm 0.11	279 \pm 2	22.9	21.8

sitive enough to conclusively detect any of our candidate companions. Six stars were bright enough to use as a background grid of reference stars compared to WD 1620-391's position. Of these six, five were distinct point sources. The sixth appears to be extended, either because it has a disk or because it is a binary. When comparing the relative position between these presumably stationary objects in six months and WD 1620-391, we measured a change in RA of 204 ± 10 mas and in Dec of 16 ± 10 mas. We derived the error based on the standard deviation of the individual measurements from the mean. Taking into account WD 1620-391's parallax motion during this period, one would expect a motion of 230 mas in RA and 28 mas in Dec assuming WD 1620-391's reported parallax of 78.85 mas (Perryman et al. 1997). Subtracting this motion leaves 26 ± 10 mas and 12 ± 10 mas from the measured motion with our reference stars, suggesting that we can detect common proper motion and common parallactic motion in a future epoch with HST and these reference stars. Since we have successfully proposed for HST time in Cycle 14 to follow up these candidates, we expect to have a long enough baseline to definitively determine if any of the candidates are physically associated.

5. LIMITS TO COMPANIONS

The main goal of this search was to detect candidate companions, but upper limits to the detection of such companions is also important for understanding the true nature of DAZ WDs, as well as the process of planet and brown dwarf formation around intermediate mass stars. To this end, in this Section we quantify our sensitivity to companions that could have been detected, in order to determine the frequency of high mass planets and brown dwarfs.

5.1. Near-IR Photometry

While direct imaging is most sensitive to companions $>0.9''$ unresolved companions could still be present for

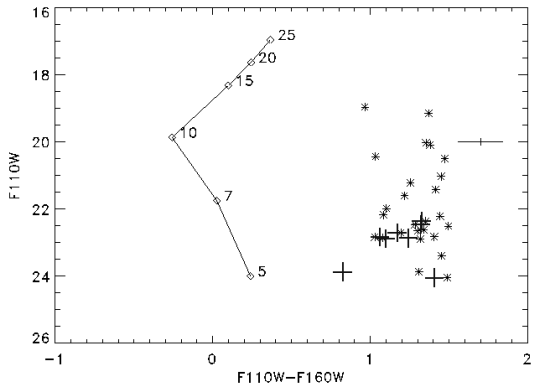


FIG. 6.— Color magnitude diagram of sources near the white dwarf WD 1620-391. Overplotted is an isochrone of 1 Gyr substellar models from Burrows et al. (2003) convolved with HST filters at 12 pc. Thick crosses are sources $<4''$ away.

some of these targets. In order to rule out companions at separations where imaging or PSF subtraction could not resolve them, we turn to the near-infrared fluxes of these objects provided by near-IR photometry, such as from 2MASS (Cutri et al. 2003). Looking in the near-IR can facilitate the discovery of cool objects around WDs (Probst & O'Connell 1982; Zuckerman & Becklin 1992; Green et al. 2000).

Our strategy was to take model values reported in the literature, generate predicted 2MASS J, H, and K_s magnitudes by using the models of Bergeron et al. (1995) and comparing J_{th} , H_{th} , and $K_{s(th)}$ with the observed magnitudes of the WDs. For our sample of white dwarfs we took model values of T_{eff} , $\log g$, and the mass from Liebert et al. (2005), Bergeron et al. (2001), and Bragaglia et al. (1995).

To compare the predicted magnitudes to those observed we took the difference of the predicted magnitudes in the 2MASS filter system J_{th} , H_{th} , and $K_{s(th)}$ and the observed magnitudes J, H, and K_s. A significant positive value would indicate an excess due to either an unseen companion or a dust disk, while a significant negative value would indicate an anomalous paucity of flux. While we used the results of DSW05 for two of our white dwarfs for the rest of our targets we used the Bergeron et al. (2001) and Bragaglia et al. (1995) samples since they provide atmospheric parameters for the remaining five white dwarfs. In general, we compared J magnitudes since WD 2326+049 has an infrared excess due to a dust disk at wavelengths longer than ~ 1.6 μ m. Excesses in J tend to be more sensitive because J band photometric errors are smaller in 2MASS. For the rest of

the targets we also checked to see if there were excesses in any of the other bands or for other targets in the sample. An excess was considered significant if it was greater than three times the measured scatter of a sample and if it was present in more than one filter.

We tested the accuracy of the three samples of WD parameters to reliably report a 3σ excess limit. We first examined the Bergeron et al. (2001) sample, which includes WD 0208+395, WD 0245+541, WD 0243-025, and WD 1257+278. Of the 150 white dwarfs we chose 146 of the sample that had reliable photometry from Bergeron et al. (2001) and converted their MKO magnitudes to 2MASS magnitudes³ to compare with our predicted magnitudes.

We neglected any object with an excess $> 3\sigma$ and recalculated the scatter in expected minus observed magnitudes, repeating the process three times. We ensured that the median values of the differences were consistent with zero. From the 146 WDs we find that the 1σ error in total of J, H, and K_s are 0.04, 0.04, and 0.05 mag. One important note is that Bergeron et al. (2001) used their JHK photometry to help fit several of the parameters that we used to generate our theoretical magnitudes, namely $\log g$ and T_{eff} . For this reason we had to be more careful interpreting these limits because it is possible the presence of a companion was “fitted out”. In this case we are placing limits to what kind of excess would have been detected by the models, rather than extrapolating from the models and looking for excesses. No objects in this sample showed a significant excess.

For WD 2326+049 and WD 1337+705 we took the sample of Liebert et al. (2005) which is a study of DA WDs from the Palomar-Green survey of UV excess sources. Of the 374 white dwarfs we chose the brightest 72 of the sample that had a $J < 15$, had unambiguous sources in 2MASS, and had reliable photometry, i.e. those objects that had quality flags of A or B in the 2MASS point source catalogue for their J magnitudes. After determining the standard deviation of the sample, we found that 1σ errors for the sample in the J, H, and K_s filters were 0.07, 0.10, and 0.15 mag, respectively. Further details of the Liebert et al. (2005) sample are presented in DSW05.

For WD 1620-391, we needed to use the sample in Bragaglia et al. (1995), using ~ 35 of the 50 WDs modeled in that work. We again picked WDs with $V < 15$, reliable 2MASS positions, and reliable photometry in the three bands. Six white dwarfs had poor photometry or incorrect distance moduli, but these errors were corrected. The final errors were calculated, resulting in 1σ errors of 0.09, 0.08, 0.15 mag for J, H, and K_s respectively. Two WDs remained with significant excess, WD 1042-690, and WD 1845+019. WD 1042-690 is a known binary system with a dM companion, and WD 1845+019 does not currently seem to be a candidate for an excess. However, its position in both the POSS and 2MASS plates based on the position given by Lanning (2000) shows that it is blended with another point source. Inspection of the POSS and 2MASS plates leaves it ambiguous whether this barely resolved object (separation $\sim 3''$) is co-moving or not, so we mark this as a potential common proper motion WD/dM pair.

TABLE 5
COMPARISON OF PREDICTED VS. 2MASS PHOTOMETRY

WD	J _{th}	H _{th}	K _{s(th)}	J	H	K _s
0208+396	13.74	13.61	13.57	13.76	13.66	13.61
0243-026	14.65	14.49	14.43	14.67	14.50	14.49
0245+541	13.86	13.61	13.47	13.86	13.67	13.58
1257+278	14.95	14.89	14.88	14.95	14.92	14.89
1337+701	13.23	13.36	13.41	13.25	13.36	13.45
1620-391	11.53	11.66	11.74	11.58	11.71	11.77
2326+049	13.13	13.19	13.22	13.13	13.08	12.69

Table 5 shows the expected 2MASS magnitudes based on the model values, and the observed magnitudes of our target white dwarfs. All of our targets fall within 1-2 σ of our expected values for all three filters, with the exception of WD 2326+049, as mentioned above.

Since none of our targets have significant excesses, we can use the 3σ limits in J to place upper limits to unresolved sources. We took the predicted J magnitudes from substellar atmosphere models, corrected for distance modulus, calculated the excess, and compared it to our sensitivity limit (Baraffe et al. 1998, 2003). Table 6 shows the unresolved companion upper limits for each target. Any companion with a mass beyond the hydrogen burning limit would have been detected for all of the target WDs.

5.2. Imaging

Schneider & Silverstone (2003) showed a reliable way to determine sensitivity of an observation with NICMOS, given the stability of the instrument. Artificial “companions” are generated with the HST PSF simulation software TINYTIM⁴ and scaled until they are recovered. These companions are inserted into the observations and used to gauge sensitivity. We adopted this strategy for our data as well. An implant was placed in the images. Two difference images were created following our procedure of PSF subtraction and then rotated and combined for maximum signal to noise. Sample images were looked at by eye as a second check that the dimmest implants could be recovered. The implants were normalized so that their total flux was equal to 1 DN/s. The normalized value was converted to a flux in Jy or a Vega magnitude by multiplying by the correct photometry constants given by the NICMOS Data Handbook. We considered an implant recovered if its scaled flux in a given aperture had a S/N of 5.

For our Gemini data, we used the PSF of WD 2326+049 as a reference for the implant. The implant was normalized to a peak pixel value of one. Scaled versions of the implants were then used to determine the final image’s sensitivity to objects at a S/N of 10, since significant flux from the PSF remained at separations $< 1''$. The relative flux of the implant with respect to the host star was measured and a corresponding MKO H magnitude was derived from the 2MASS H magnitude to give a final apparent magnitude sensitivity. For our Gemini images we checked sensitivity starting at a distance of ~ 3 times the FWHM of WD 2326+049, or $0.22''$,

³ http://www.ipac.caltech.edu/2mass/releases/allsky/doc/sec6_4b.html ⁴ <http://www.stsci.edu/software/tinytim/tinytim.html>

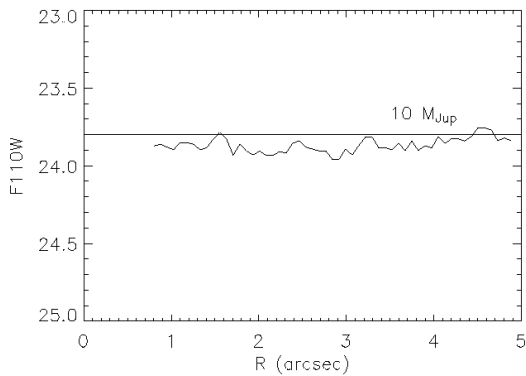


FIG. 7.— Sensitivity at 5σ to point sources in F110W around the WD WD 0208+395. The WDs F110W magnitude is ~ 13.8 , giving a contrast of 10 magnitudes at $1''$. Overplotted is the magnitude of a $10 M_{Jup}$ planet 3.2 Gyr old at the distance of WD 0208+395 from the models of Burrows et al. (2003).

out to $1''$.

Figure 7 shows an example of the azimuthally averaged 5σ sensitivity for WD 0208+395. In order to determine the total age of WD 0208+395 as well as each other system, we took each inferred mass and derived an initial mass by the relation $10.4 \ln[(M_{WD}/M_{\odot})/0.49] M_{\odot}$, the results of which are given in Table 1 (Wood 1992). The mass then gave a main sequence lifetime given by $t_{MS}^{-2.5}$ Gyr, which gave a total age when coupled with the inferred cooling time from the same models used for our 2MASS photometry. With a total estimated system age of ~ 3 Gyr for WD 0208+395, we overplotted the lowest companion mass detectable, using the models of Burrows et al. (2003). These models differ slightly from the models of Baraffe et al. (2003), used for our 2MASS excess limits. The Burrows et al. (2003) models tend to predict dimmer near-IR magnitudes for the planetary mass objects, but converge with the Baraffe et al. (2003) models for higher masses. It is therefore possible that we are sensitive to objects $\sim 1-2 M_{Jup}$ less massive if the Baraffe et al. (2003) models are correct. Table 6 has the mass limits for each WD for separations $> 0.9''$.

6. DISCUSSION

We can use Table 6 and the results of our excess limits to draw some broad conclusions from this search. The combination of the 2MASS excess determinations and the HST imaging create the most sensitive search for planets around WDs to date. The sensitivity achieved could easily have detected an object $> 10 M_{Jup}$ at separations > 30.6 AU, with the closest detection possible at 9.3 AU. Taking into account that any primordial companions' semi-major axis would have expanded by a factor of M_i/M_f , we can infer the closest primordial separation these objects would have had if they had been detected. Taking the values of Table 1 for M_i and M_f and using our minimum projected angular separation, we find that any object that formed at > 10 AU could have been detected, assuming that there were no forces that retarded expansion. Forces that could retard expansion would be due to tidal interactions with the giant star. However, this effect should be minimal at initial distances of 10 AU (Rasio et al. 1996).

We can also make some initial comments about the origin of DAZ white dwarfs. Given the upper limits on unresolved companions, we can infer the plausibility of one of the possible explanations for the DAZ phenomenon. The problems with ISM accretion have been documented extensively in the work of Zuckerman et al. (2003) and Aannestad et al. (1993). In Zuckerman et al. (2003) they noted that a large fraction of DA/dM objects had metal absorption lines in their atmospheres, and inferred that other DAZs may be the result of unseen companions. If this scenario is true, then for each of these objects, the maximum companion mass plausible is $< 70 M_{Jup}$.

If the explanation for DAZs is due to close brown dwarf companions, the frequency of DAZs is at odds with the frequency of DAZs one would predict based on radial velocity surveys. These surveys find that $\sim 0.5\%$ of stars have brown dwarfs with semi-major axes < 3 AU (Marcy & Butler 2000). One would expect 0.5% or less of field DAs to be DAZs based on the radial velocity result. The only possible counter explanation is that brown dwarf formation at these radii is ~ 40 times more efficient for higher mass main sequence stars. Radial velocity surveys of G giants are too young to reliably estimate the fraction of brown dwarf companions in orbits wider than ~ 1 AU, but none have yet been found in ~ 100 stars (Sato et al. 2003).

We can compare our results with those of radial velocity surveys. By comparing both results we can look at predictions for the frequency of massive planets around a random sample of stars and around stars that possess planetary systems. Since the numbers are small, we will merely look at percentages and assume that they are constant as a function of distance and central stellar mass, clearly naive assumptions. Since 5% of field stars have planetary systems, we need to estimate how many would have planets massive enough to be detectable by our observations. Of the 118 known planetary systems in orbit around solar type stars, ~ 6 have companions with $M_{\sin i} > 10 M_{Jup}$ ⁵. The frequency of such planets amongst stars already bearing one or more planets is then $\sim 5\%$, leading to an overall probability of 0.25% of all field stars possessing a planet that we could have detected. Assuming Poisson statistics, to have a 50% chance at detecting one or two planets would require a sample of 400 WDs with ages ~ 3 Gyr. The limit sensitive radial velocity studies have on A stars can be partially circumvented by searching G giants for radial velocity variations (Sato et al. 2003). G giants are typically intermediate mass stars, although field giants tend to have larger uncertainties in their mass compared to the main sequence stars in other radial velocity surveys. As of the results published in Sato et al. (2003), one planetary object with $M_{\sin i} = 6-10 M_{Jup}$ and semi-major axis ~ 1 AU had been detected in a sample of ~ 100 targets. The implied frequency of $\sim 1\%$ would mean a slightly more favorable chance to find one planet in a sample of ~ 100 WDs. If DAZs do not preferentially harbor planetary systems, it will be a long search if we only focus on them. Any search should include DAZs, but also focus on a larger sample.

Let us now consider the possibility that DAZs do pref-

⁵ <http://www.obspm.fr/encycl/encycl.html>

TABLE 6
UPPER LIMITS TO COMPANIONS

WD	Excess Limit (m _J) (J)	Mass (M _{Jup})	Sensitivity > 0.9'' (F110W)	Mass (M _{Jup})
0208+396	16.2	48	23.9	10
0243-026	17.5	51	24.1	10
0245+541	16.2	53	23.5	18
1257+278	17.0	40	23.8	14
1337+701	14.9	70	23.4	14
1620-391	12.9	61	22.9	7
2326+049	14.8	39	23.3	6

entially harbor planetary systems, and based on our detection limits estimate how many DAZs would need to be observed. Since we could detect > 10 M_{Jup} objects and $\sim 5\%$ of field stars with planetary systems have objects that massive, we can infer that 5% of DAZs could have planets that could have been detected. If DAZs (and also DZs or helium white dwarfs with metal absorption) are indeed good markers for planetary systems, one would need a sample of 20 WDs to have a 50% chance to detect a massive planet. To date ~ 34 DAZs are known. Currently the estimated fraction of apparent single WDs that are DAZs is $\sim 20\%$. If they all harbor planets, this estimated fraction implies a much higher frequency of planets than that measured by radial velocity surveys. However, radial velocity surveys are starting to detect longer period systems, which may have a higher frequency of formation and better represent the type of population that would cause a DAZ (Jones et al. 2002).

There are then two approaches to continuing the search-increasing the sample size and increasing the sensitivity of a search. In the short term a large sample of WDs must be observed, since the probable frequency of massive planets among WDs that harbor a planetary system is small. Future observatories such as the James Webb Space Telescope should have an easier time detecting Jovian and sub-Jovian planets, which will hopefully resolve the origin of DAZs. Such future observations will determine whether DAZs are ultimately useful for planetary studies, including spectroscopy.

The discovery of candidate planetary mass companions demonstrates that this limited survey was sensitive to planets. These results show that if massive planets were present around these WDs we would have detected them. Even with a small sample, limits can be placed on the frequency of massive planets in orbit around stars more massive than the Sun, and begin to observationally address the question of planet formation efficiency

vs. spectral type. Ideally, the next step would be to expand the sample of WDs studied and to probe to lower masses, where the planetary mass function peaks (~ 1 M_{Jup}). High spatial resolution and sensitivity missions like JWST would most likely be able to detect such objects around nearby WDs.

We would like to gratefully acknowledge Al Shultz and Glenn Schneider for helpful conversations about coronagraphy with NICMOS, and Chad Trujillo and Joe Jensen for critical help with the inner workings of Altair and the reduction of Altair imaging data.

Based on observations made with the NASA/ESA Hubble Space Telescope, obtained at the Space Telescope Science Institute, which is operated by the Association of Universities for Research in Astronomy, Inc., under NASA contract NAS5-26555. These observations are associated with program #9834. Also based on observations obtained at the Gemini Observatory, which is operated by the Association of Universities for Research in Astronomy, Inc., under a cooperative agreement with the NSF on behalf of the Gemini partnership: the National Science Foundation (United States), the Particle Physics and Astronomy Research Council (United Kingdom), the National Research Council (Canada), CONICYT (Chile), the Australian Research Council (Australia), CNPq (Brazil) and CONICET (Argentina). Near-IR Photometry obtained as part of the Two Micron All Sky Survey (2MASS), a joint project of the University of Massachusetts and the Infrared Processing and Analysis Center/California Institute of Technology, funded by the National Aeronautics and Space Administration and the National Science Foundation. S.S. also acknowledges funding under the Pennsylvania State University Astrobiology Research Consortium (PSARC).

REFERENCES

Aannestad, P. A., Kenyon, S. J., Hammond, G. L., & Sion, E. M. 1993, AJ, 105, 1033

Alcock, C., Fristrom, C. C., & Siegelman, R. 1986, ApJ, 302, 462

Althaus, L. G. & Benvenuto, O. G. 1998, MNRAS, 296, 206

Bakos, G. Á., Sahu, K. C., & Németh, P. 2002, ApJS, 141, 187

Baraffe, I., Chabrier, G., Allard, F., & Hauschildt, P. H. 1998, A&A, 337, 403

Baraffe, I., Chabrier, G., Barman, T. S., Allard, F., & Hauschildt, P. H. 2003, A&A, 402, 701

Bergeron, P., Leggett, S. K., & Ruiz, M. T. 2001, ApJS, 133, 413

Bergeron, P., Wesemael, F., Lamontagne, R., Fontaine, G., Saffer, R. A., & Allard, N. F. 1995, ApJ, 449, 258

Bragaglia, A., Renzini, A., & Bergeron, P. 1995, ApJ, 443, 735

Burgasser, A. J., Kirkpatrick, J. D., McElwain, M. W., Cutri, R. M., Burgasser, A. J., & Skrutskie, M. F. 2003, AJ, 125, 850

Burleigh, M. R., Clarke, F. J., & Hodgkin, S. T. 2002, MNRAS, 331, L41

Burrows, A., Sudarsky, D., & Hubeny, I. 2004, ApJ, 609, 407

Burrows, A., Sudarsky, D., & Lunine, J. I. 2003, ApJ, 596, 587

Cutri, R. M., et al. 2003, VizieR Online Data Catalog, 2246, 0

Debes, J. H., Ge, J., & Ftaclas, C. 2005a, in preparation

Debes, J. H. & Sigurdsson, S. 2002, ApJ, 572, 556

Debes, J. H., Sigurdsson, S., & Woodgate, B. 2005b, (ApJ, submitted)

Delfosse, X., Forveille, T., Mayor, M., Perrier, C., Naef, D., & Queloz, D. 1998, *A&A*, 338, L67

Dupuis, J., Fontaine, G., Pelletier, C., & Wesemael, F. 1992, *ApJS*, 82, 505

—. 1993a, *ApJS*, 84, 73

Dupuis, J., Fontaine, G., & Wesemael, F. 1993b, *ApJS*, 87, 345

Ford, E. B., Havlickova, M., & Rasio, F. A. 2001, *Icarus*, 150, 303

Forveille, T., et al. 2004, *A&A*, 427, L1

Fraquelli, D. A., Schultz, A. B., Bushouse, H., Hart, H. M., & Vener, P. 2004, *PASP*, 116, 55

Gianninas, A., Dufour, P., & Bergeron, P. 2004, *ApJ*, 617, L57

Gladman, B. 1993, *Icarus*, 106, 247

Grady, C. A., Woodgate, B., Bruhweiler, F. C., Boggess, A., Plait, P., Lindler, D. J., Clampin, M., & Kalas, P. 1999, *ApJ*, 523, L151

Graham, J. R., Matthews, K., Neugebauer, G., & Soifer, B. T. 1990, *ApJ*, 357, 216

Green, P. J., Ali, B., & Napiwotzki, R. 2000, *ApJ*, 540, 992

Griffin, R. E. M., David, M., & Verschueren, W. 2000, *A&AS*, 147, 299

Hawley, S. L., et al. 2002, *AJ*, 123, 3409

Hill, G. 1886, *Acta Mathematica*, 8, 1

Holberg, J. B., Bruhweiler, F. C., & Andersen, J. 1995, *ApJ*, 443, 753

Holland, W. S., et al. 1998, *Nature*, 392, 788

Hutchings, J. B., Stoesz, J., Veran, J.-P., & Rigaut, F. 2004, *PASP*, 116, 154

Ignace, R. 2001, *PASP*, 113, 1227

Jayawardhana, R., Fisher, S., Hartmann, L., Telesco, C., Pina, R., & Fazio, G. 1998, *ApJ*, 503, L79+

Jeans, J. H. 1924, *MNRAS*, 85, 2

Jones, H. R. A., Paul Butler, R., Marcy, G. W., Tinney, C. G., Penny, A. J., McCarthy, C., & Carter, B. D. 2002, *MNRAS*, 337, 1170

Jura, M. 2003, *ApJ*, 584, L91

Lada, C. J. & Lada, E. A. 2003, *ARA&A*, 41, 57

Lanning, H. H. 2000, *VizieR Online Data Catalog*, 2231, 0

Liebert, J., Bergeron, P., & Holberg, J. B. 2005, *ApJS*, 156, 47

Marcy, G. W. & Butler, R. P. 2000, *PASP*, 112, 137

Parriott, J. & Alcock, C. 1998, *ApJ*, 501, 357

Patterson, J., Zuckerman, B., Becklin, E. E., Tholen, D. J., & Hawarden, T. 1991, *ApJ*, 374, 330

Perryman, M. A. C., et al. 1997, *A&A*, 323, L49

Probst, R. G. & O'Connell, R. W. 1982, *ApJ*, 252, L69

Rasio, F. A., Tout, C. A., Lubow, S. H., & Livio, M. 1996, *ApJ*, 470, 1187

Sato, B., et al. 2003, *ApJ*, 597, L157

Schneider, G. & Silverstone, M. D. 2003, in *High-Contrast Imaging for Exo-Planet Detection*. Edited by Alfred B. Schultz. Proceedings of the SPIE, Volume 4860, pp. 1-9 (2003)., 1-9

Setiawan, J., et al. 2005, *ArXiv Astrophysics e-prints*

Sigurdsson, S., Richer, H. B., Hansen, B. M., Stairs, I. H., & Thorsett, S. E. 2003, *Science*, 301, 193

Tremaine, S. 1993, in *ASP Conf. Ser.* 36: *Planets Around Pulsars*, 335-344

van Altena, W. F., Lee, J. T., & Hoffleit, E. D. 2001, *VizieR Online Data Catalog*, 1238, 0

Weinberger, A. J., Becklin, E. E., Schneider, G., Smith, B. A., Lowrance, P. J., Silverstone, M. D., Zuckerman, B., & Terrile, R. J. 1999, *ApJ*, 525, L53

Wolszczan, A. & Frail, D. A. 1992, *Nature*, 355, 145

Wood, M. A. 1992, *ApJ*, 386, 539

Zuckerman, B. & Becklin, E. E. 1992, *ApJ*, 386, 260

Zuckerman, B., Koester, D., Reid, I. N., & Hünsch, M. 2003, *ApJ*, 596, 477

Zuckerman, B. & Reid, I. N. 1998, *ApJ*, 505, L143